

## Structural investigation of water and aqueous solutions by Raman spectroscopy\*

F. Rull<sup>‡</sup>

*Unidad Asociada al Centro de Astrobiología, INTA-CSIC; Cristalografía y Mineralogía, Facultad de Ciencias, Universidad de Valladolid, Valladolid, Spain*

**Abstract:** In the context of a long study of the dynamical properties of water and inorganic aqueous solutions using infrared (IR) and Raman spectroscopy, we present here recent results of the influence of salt concentration on the dynamics of water molecules. The main systems studied were salts of  $X_n Y_m$  type (where  $X = \text{Li}^+, \text{Na}^+, \text{K}^+, \text{Rb}^+, \text{Cs}^+, \text{Mg}^{2+}, \text{Zn}^{2+}$  and  $Y = \text{Cl}^-, \text{ClO}_4^-, \text{NO}_3^-, \text{SO}_4^{2-}$ ).

The whole spectrum reflects the molecular and ionic interactions between solvent molecules and solvent–solute and solute–solute molecules. Nevertheless, each spectral region supplies different information about these intermolecular interactions.

The strong modifications in intensity and band profile undergone by the  $\nu(\text{OH})$  band depends mainly on the nature of anions while cations have a weak influence. A picture of these different situations in a particular salt solution needs the support of a model of the dynamic structure of the water solvent. A discussion of the current state of the dynamical models of liquid water and new ideas on water dynamics are presented on the basis of the results obtained from the study of internal OH/OD vibrations of water in diluted mixtures of  $\text{D}_2\text{O}/\text{H}_2\text{O}$ .

Finally, a comparative analysis of the influence on the dynamics of water molecules under the concentration of perchlorate and chloride salts of monovalent cations in water and isotopic  $\text{D}_2\text{O}/\text{H}_2\text{O}$  mixtures was undertaken using Raman spectroscopy.

### INTRODUCTION

Among the numerous methods used to investigate the structural properties of water and aqueous solutions, those based on X-ray diffraction (XRD) or neutron diffraction, together with spectroscopic methods, have been preferred as they give direct information about the static (pair correlation functions) or dynamic structure of the liquid. During the last four decades, both techniques generated a huge amount of results, which have been in their turn tested against more and more sophisticated theoretical models using computer simulation [1–6].

With only a few exceptions, most of the structural models proposed from the early work of Bernal and Fowler [7] for liquid water fell into one of the two classical models, that is, continuum or mixture models [8–10]. Continuum models received particular attention in computer simulation during the 1970s and 1980s, and a large number of results have been used to support the idea of a disordered network of hydrogen bonds as the base of the structural, dynamical, and physical properties of water [11–14].

---

\*Lecture presented at the 10<sup>th</sup> International Symposium on Solubility Phenomena, Varna, Bulgaria, 22–26 July 2002. Other lectures are published in this issue, pp. 1785–1920.

<sup>‡</sup>E-mail: rull@fmc.uva.es

Nevertheless, in the last few years, the alternative idea has gained favor and water has been considered a mixture in several ways: a two-state system [15,16], a four-structural components system [17], or it is simulated on the basis of an equilibrium between different cluster structures, mainly dodecahedral and icosahedral [18,19]. In most of these models, two main local structural situations are generally invoked—a distorted tetrahedral pattern and some amount of interstitial water molecules. The last term means classically unbonded or weakly hydrogen-bonded water molecules sitting in the tetrahedrally bonded network.

Vibrational spectroscopic techniques and, particularly, Raman spectroscopy are very well suited for studying these local structures, provided the spectrum is mainly sensitive to short-range interactions affecting the probe oscillators. Nevertheless, the  $\nu(\text{OH})$  band of liquid water and aqueous solutions shows a very complex envelope to which contribute the wide distribution of O–O distances and HOH bonds, the intra- and intermolecular couplings, and the possibility of Fermi resonance between the first harmonic of the HOH deformation mode and the fundamental  $\nu(\text{OH})$  [20,21]. Isotopic mixtures of  $\text{D}_2\text{O}$  in  $\text{H}_2\text{O}$  minimized most of these effects, and in the dilute range (i.e., less than 10 % of one component), HOD molecules are the main part of the chemical species, which are also quite free from intermolecular couplings. In this case, the OD or OH oscillators vibrate only in accord with their local surroundings, and different components can be associated with different local structures in the liquid [22].

In the context of a detailed study of the dynamical properties of water and inorganic aqueous solutions related to the influence of salt concentration on the dynamics of water molecules and polyatomic anions using IR and Raman spectroscopy, we present here recent results on the influence of salt concentration on the  $\nu(\text{OH})$  and  $\nu(\text{OD})$  bands at room temperature. The main systems studied were salts of  $X_n Y_m$  type (where  $X = \text{Li}^+, \text{Na}^+, \text{K}^+, \text{Rb}^+, \text{Cs}^+, \text{Mg}^{2+}, \text{Zn}^{2+}$  and  $Y = \text{Cl}^-, \text{ClO}_4^-, \text{NO}_3^-, \text{SO}_4^{2-}$ ). In this work, we will focus on Raman results obtained from aqueous solutions of  $\text{LiCl}$  and  $\text{LiClO}_4$  salts in  $\text{D}_2\text{O}/\text{H}_2\text{O}$  mixtures.

## EXPERIMENTAL

Standard aqueous solutions were prepared from analytical grade reagents. The deuteration effect was performed using  $\text{D}_2\text{O}$  of 99.9 % purity. The concentration was calculated in molal units in all cases. Raman spectra were taken in two modes, the classical  $90^\circ$  configuration using polarized light and the  $180^\circ$  configuration in depolarized light. In both cases, the exciting radiation at 514.5 nm is provided by an ionized Argon laser (SpectraPhysics, model 2020). The output laser power ranged between 200 and 400 mW.

In the  $90^\circ$  configuration, Raman spectra were recorded with a Ramanor HG2S spectrophotometer coupled to a computer system. The vertically polarized laser beam was focused in a  $2\text{-cm}^3$  quartz thermostated cell, and  $I_{\nu\nu}$  and  $I_{\nu\text{h}}$  components were analyzed.

In the  $180^\circ$  configuration, the Raman probe was a Labram (Dilor) coupled to a microscope. Objectives used were  $20\times$  and  $50\times$ . Integration time was around 100 s for calibration solutions and chosen in order to get an intensity between half and  $2/3$  of the maximum intensity accepted by the charge-coupled device (CCD) detector. For each series of solution, a spectrum of pure water was made.

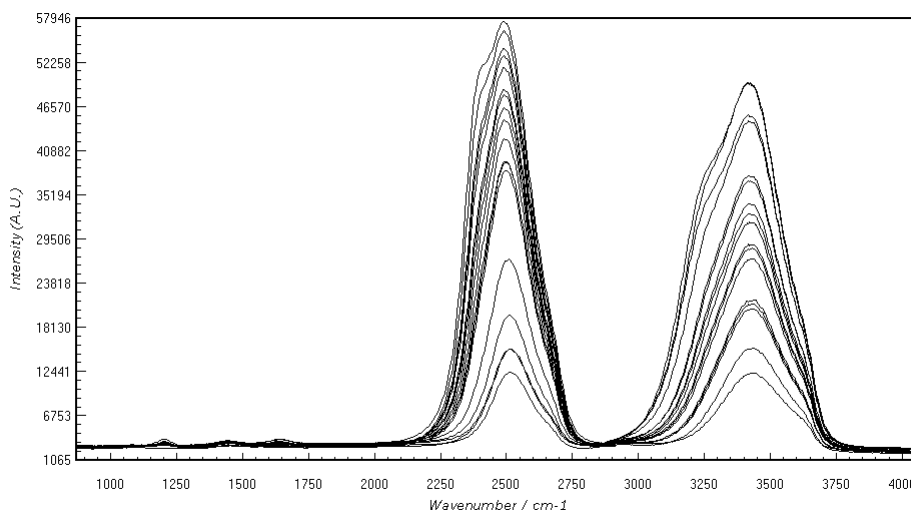
Spectra were computer-processed in several ways and corrected by the baseline in order to perform appropriate-difference spectra. The true shape in the OD/OH stretching region was obtained by correcting intensity by the internal field effect, and the four-power correction  $[(\nu_L - \nu)/\nu]^4$  where  $\nu_L$  is the absolute wavenumber of the exciting radiation. Self-deconvolution by Fourier techniques, as well as fitting methods using least square and simplex algorithms, were also used [23].

## RESULTS AND DISCUSSION

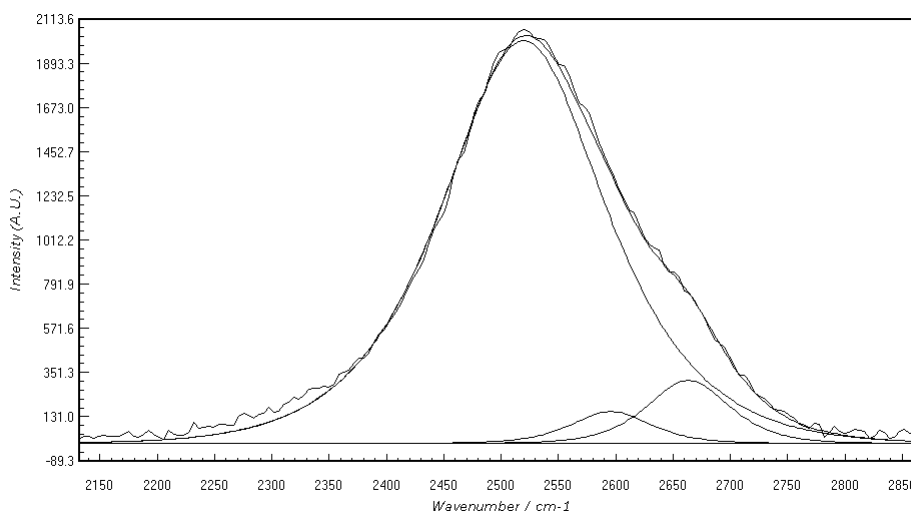
### D<sub>2</sub>O–H<sub>2</sub>O mixtures

Figure 1 shows the full-range spectra of internal vibrations of a D<sub>2</sub>O–H<sub>2</sub>O mixture as a function of the relative concentration. As can be easily seen at low concentrations of H<sub>2</sub>O or D<sub>2</sub>O,  $\nu(\text{OH})$  and  $\nu(\text{OD})$  bands show a simplified profile that has been the object of interest for a number of authors [21,24–27]. Two components at 2520 and 2666 cm<sup>-1</sup> for D<sub>2</sub>O and two at 3420 and 3630 cm<sup>-1</sup> for H<sub>2</sub>O are clearly identified.

Nevertheless, a detailed band profile analysis of the  $\nu(\text{OD})$  band using self-deconvolution procedures and fitting methods in the whole range 1000–4000 cm<sup>-1</sup> to include the contributions of the weak bands (see details in Fig. 7) allows identification of a third component at 2597 cm<sup>-1</sup> (Fig. 2). The evo-



**Fig. 1** Raman spectra of H<sub>2</sub>O/D<sub>2</sub>O isotopic mixtures. Relative concentration ranges between 5 and 95 %.



**Fig. 2** Band fitting of the  $\nu(\text{OD})$  band of HOD at relative concentration 2 % D<sub>2</sub>O in H<sub>2</sub>O.

lution of the band parameters of these components as a function of  $D_2O$  concentration in  $H_2O$  in the range up to the mole fraction  $x(D_2O) = 0.4$  is shown in Figs. 3 and 4.

From Fig. 4, the evolution of the relative intensity of each component can be deduced, and the results show that all three are almost constant with values 90.6, 2.4, and 6.9 %, respectively, for 2520, 2597, and 2666  $cm^{-1}$  bands. These values are consistent with the previous ones of Clarke and Glew [28] from IR absorptivity measurements, although the authors only used two components for the  $\nu(OD)$  profile.

Wavenumbers are also constants for all three bands up to  $x(D_2O) = 0.1$  and only decreases appreciably as a function of  $D_2O$  concentration for the main component at 2520  $cm^{-1}$ .

This can be interpreted as the effect of intermolecular interactions, and above  $x(D_2O) = 0.4$ , also, the low wavenumber component around 2380  $cm^{-1}$  is clearly seen. This component arises mainly from

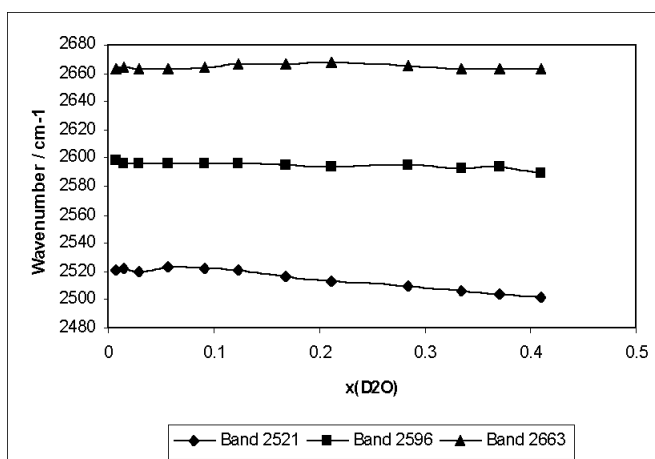


**Fig. 3** Dependence with  $D_2O$  mole fraction of the band position of the three components found by deconvolution analysis in the  $\nu(OD)$  stretching band.

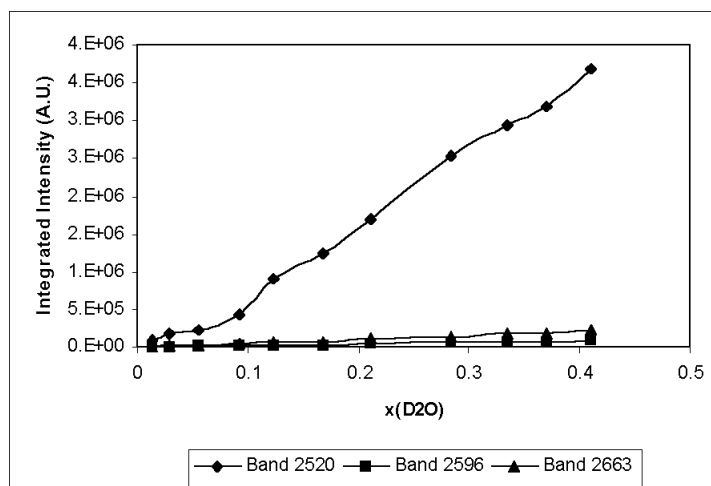


**Fig. 4** Dependence with  $D_2O$  mole fraction of the integrated intensity of the three components of  $\nu(OD)$  stretching band.

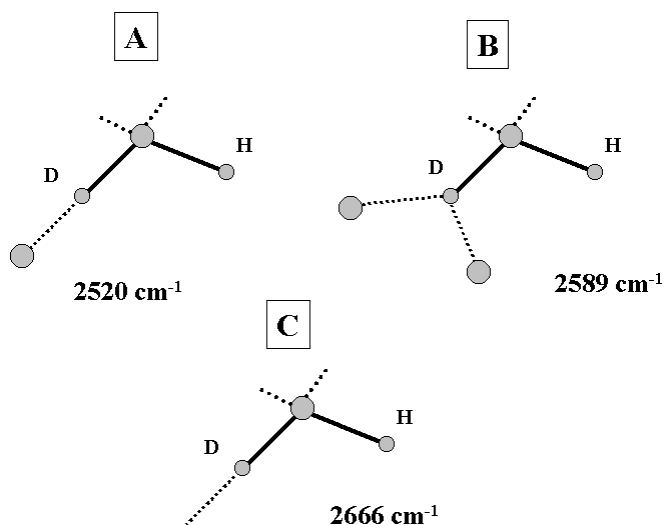


**Fig. 5** Possible local configurations of HOD molecules in a structural unit of liquid water and their assigned wavenumbers in the spectrum. (A) O–D in a linear H-bond configuration; (B) O–D in a bifurcated H-bond; and (C) O–D in interstitial position or like-free H-bond.

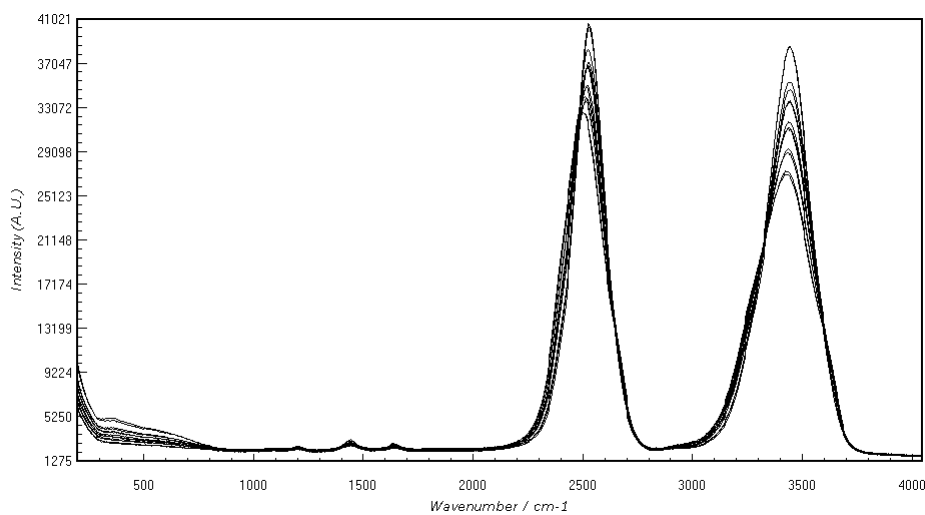
the vibrations of  $\text{H}_2\text{O}\cdots\text{HOH}\cdots\text{OH}_2$  multimers in the bulk water in which inter- and intramolecular couplings, as well as Fermi resonance effects, are possible [20,21].

These results strongly support the mixture model. Nevertheless, the assignment of the bands is inconsistent with a two-state model. We propose a model as presented in Fig. 5 in which three distinct local situations can be envisaged for uncoupled OD oscillators: one with a linear H-bond in a tetrahedral-like configuration ( $2520\text{ cm}^{-1}$ ), the second, in a bifurcated H-bond configuration ( $2597\text{ cm}^{-1}$ ), and the third corresponding to the “interstitial”, very weak or non-H-bonded OD oscillators ( $2666\text{ cm}^{-1}$ ). Note in this figure, we do not distinguish different situations affecting the lone pairs of the reference molecule. In our opinion, these have very little effect on the OH frequency of vibration and appear only as perturbations of the observed bands.

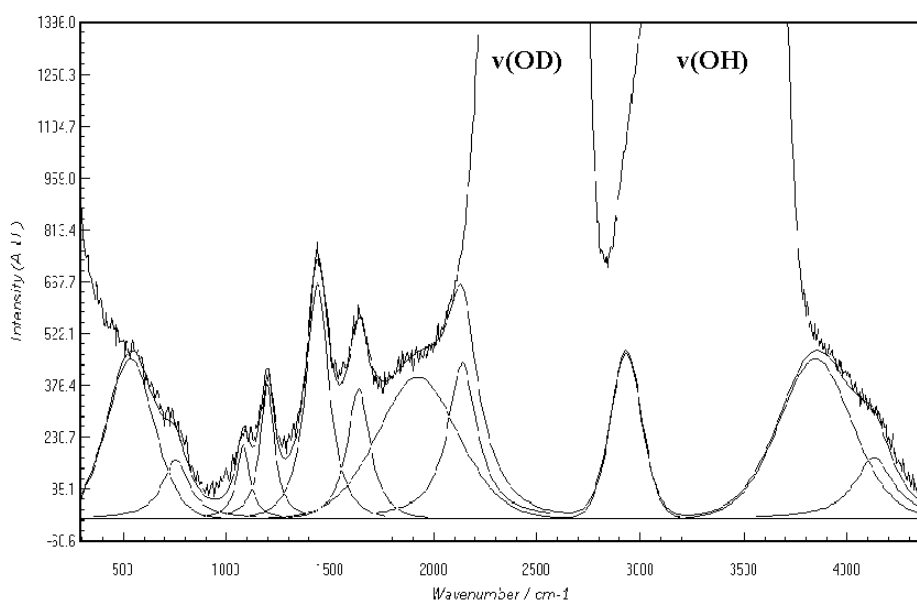
The bifurcated H-bond (BHB) was proposed several years ago by Giguère [29] as a consequence of the experimental diffraction feature  $\text{H}\cdots\text{O}$  at  $2.3\text{ \AA}$  and was assigned to the  $3420\text{ cm}^{-1}$  band in the Raman spectrum of pure water. Further evidence of the BHB has been recently shown by molecular dynamics computer simulation [30]. Nevertheless, the difficulty in accepting the assignment of Giguère to the  $3420\text{ cm}^{-1}$  OH band ( $2520\text{ cm}^{-1}$  in OD) arises from the fact that the main component in the Raman spectrum of the diluted  $\text{H}_2\text{O}$  case corresponds well to the  $3420\text{ cm}^{-1}$  band and seems unlike that of almost all the OH bonds involved in bifurcated H-bonds. Moreover, as our results show, the BHBs must be related to interstitial H-bonds in some way, providing the existence of a free OH, which needs the counterpart lone-pair to be bonded.

### Effect of salt concentration on the $\nu(\text{OD})/\nu(\text{OH})$ bands

Figure 6 shows the evolution of the Raman spectrum of a mixture 1:1 as a function of LiCl concentration in the range 0.25 to 8 m. The choice of the 1:1 isotopic mixture instead of a diluted mixture was due to the aim of comparing simultaneously the salt effect in  $\nu(\text{OD})$  and  $\nu(\text{OH})$  bands, even though the amount of both  $\text{D}_2\text{O}$ , HDO and  $\text{H}_2\text{O}$  leads to some inter- and intramolecular couplings that complicate the spectrum.



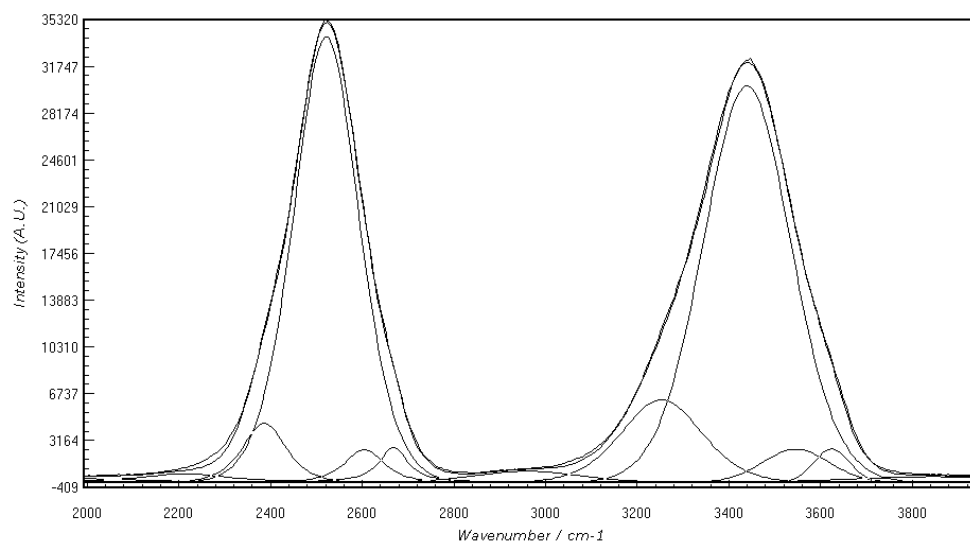
**Fig. 6** Raman spectra of LiCl solutions in 1:1 D<sub>2</sub>O/H<sub>2</sub>O mixture (concentration range 0.25–8 m).



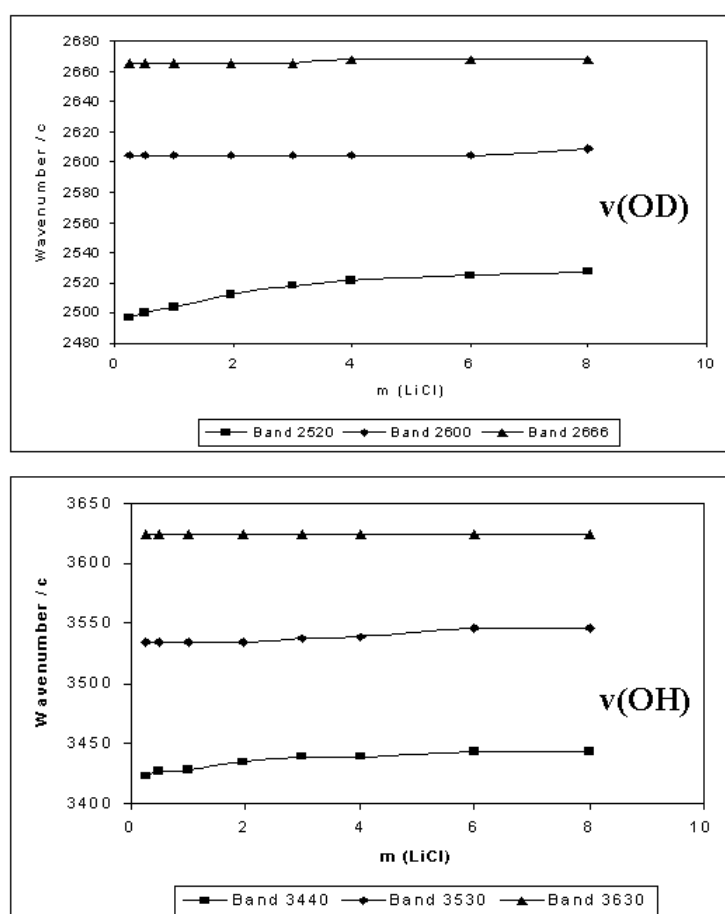
**Fig. 7** Band profile analysis of the spectral background in a LiCl solution 4 m in D<sub>2</sub>O /H<sub>2</sub>O 1:1. Bands arise from Li–O(H/D)<sub>2</sub> vibrational modes; O(H/D)<sub>2</sub> vibrational and internal bending modes and combinations bands.

Figure 7 show the details of the band components analysis performed to fit the spectral background. This procedure is necessary if accurate intensity calculations are to be performed in the v(OD)/v(OH) bands. Its influence in the overall intensity is clear, and it is noticeable that most of the previous analysis of this spectral region lacks this precise background, which is in fact a physical baseline correction [31].

In Fig. 8, the fitting results are shown for the 4-m solution in which clearly four bands are present in both OD and OH stretching regions. These bands are exactly the four components found in the pure D<sub>2</sub>O/H<sub>2</sub>O, in which only the 2380 cm<sup>-1</sup> band is absent in the diluted case because its origin is



**Fig. 8** Band component analysis of  $\nu(\text{OD})$  and  $\nu(\text{OH})$  band profiles in LiCl solution 3 m in  $\text{D}_2\text{O}/\text{H}_2\text{O}$  1:1 mixture.



**Fig. 9** Wavenumber dependence of the components of  $\nu(\text{OD})$  and  $\nu(\text{OH})$  bands with LiCl concentration in a  $\text{D}_2\text{O}/\text{H}_2\text{O}$  mixture 1:1.

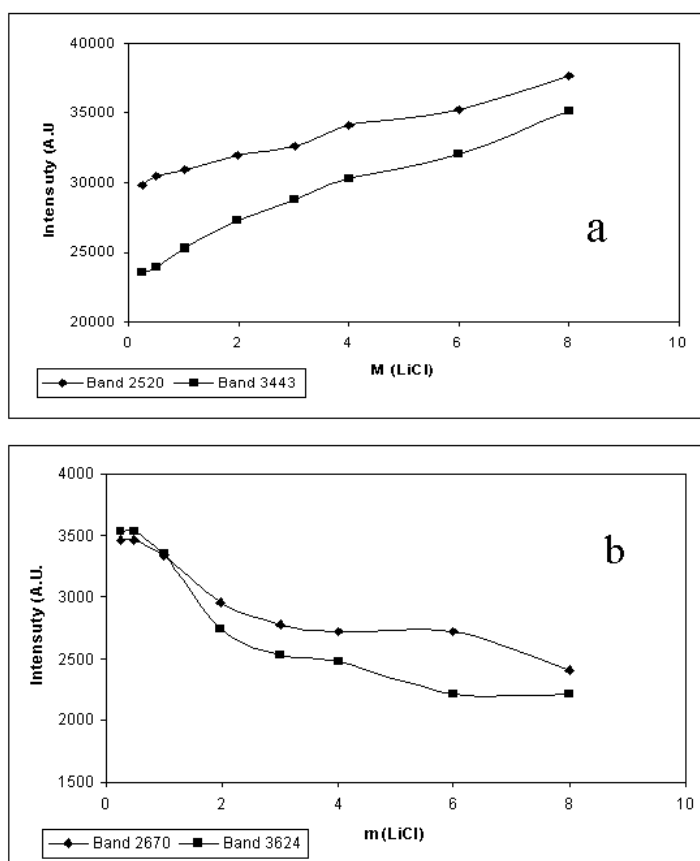


**Fig. 10** Evolution with LiCl salt concentration of the intensities of the  $\nu(\text{OD})$  and  $\nu(\text{OH})$  main components; (a)  $\nu(\text{OD})/\nu(\text{OH})$  linear H-bonds; (b) non-bonded OD/OH.

related to the vibration of intra- and intermolecular coupled oscillators of  $\text{D}_2\text{O}$  and  $\text{H}_2\text{O}$  species, as mentioned above.

The effect of LiCl concentration on these components can be followed in Figs. 9 and 10. Figure 9 shows the evolution of band positions. The components assigned to “linear” and “bifurcated” hydrogen-bonded OD/OH oscillators increase their wavenumber as concentration rises, while the component assigned to “interstitial” or free OD/OH oscillators remains almost constant. Also, the band assigned to “linear” H-bonds increases in intensity at the expense of “interstitial” 2666 and 2380  $\text{cm}^{-1}$  bands, respectively (see Fig. 6).

This can be interpreted as the result of the combined effect of  $\text{Li}^+$  and  $\text{Cl}^-$  ions.  $\text{Li}^+$  is a strong hydrating cation that disturbs the local tetrahedral-like H-bond configurations, while  $\text{Cl}^-$  is a medium H-bond acceptor with an interaction energy not far from the  $\text{OH}\cdots\text{O}$  energy. In consequence, the bands at 2380, 2589, and 2666  $\text{cm}^{-1}$  decrease in intensity, and the band at 2520  $\text{cm}^{-1}$  increases. The same trend is observed in the OH stretching region, as shown in Fig. 10.

Figure 11 shows the effect of  $\text{LiClO}_4$  salt concentration in the spectrum of  $\text{D}_2\text{O}/\text{H}_2\text{O}$  1:1 mixture, while Fig. 12 presents the band component analysis performed at 3-m concentration. A completely different pattern than in the LiCl case is observed. The band at 2520  $\text{cm}^{-1}$  (3430  $\text{cm}^{-1}$  in OH) decreases in intensity, while the band at 2666  $\text{cm}^{-1}$  (3630  $\text{cm}^{-1}$  in OH) increases (Fig. 13). Also, the shoulder at 2380  $\text{cm}^{-1}$  decreases in intensity. This results from the substitution of  $\text{Cl}^-$  by  $\text{ClO}_4^-$  ions, which are well

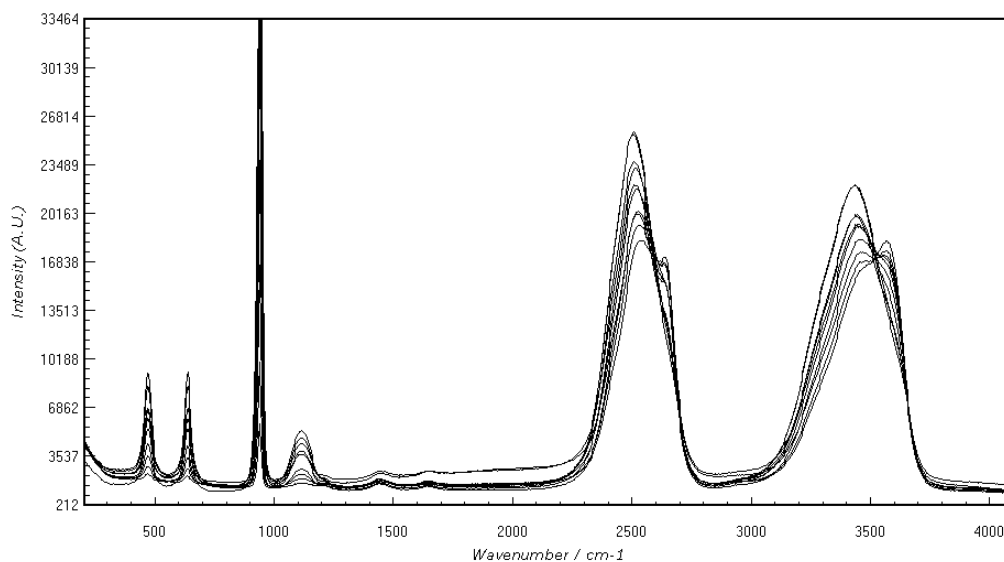


**Fig. 11** Raman spectra of  $\text{LiClO}_4$  solutions in 1:1  $\text{D}_2\text{O}/\text{H}_2\text{O}$  mixture (concentration range 0.125–4.7 m).

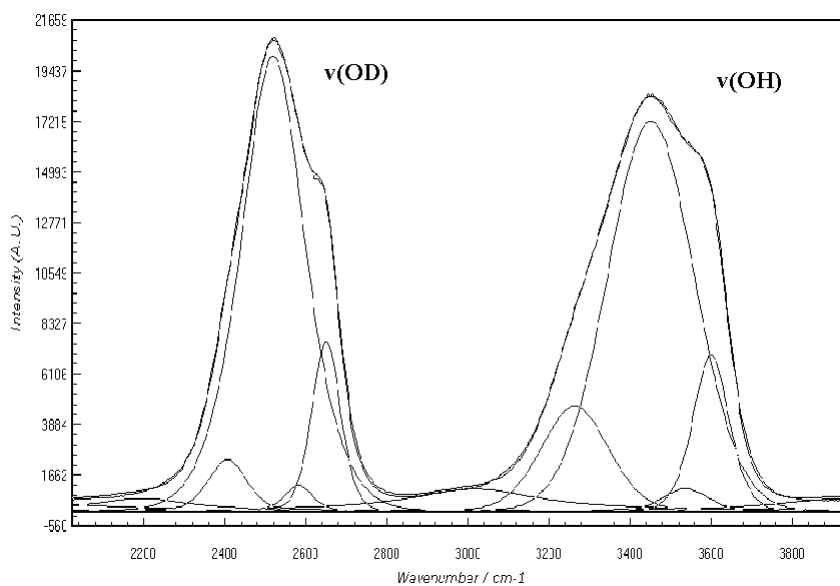


**Fig. 12** Band component analysis of  $\nu(\text{OD})$  and  $\nu(\text{OH})$  band profiles in  $\text{LiClO}_4$  solution 2.5 m in  $\text{D}_2\text{O}/\text{H}_2\text{O}$  1:1 mixture.

known to have a very weak interaction with water molecules that modify the oscillators' distribution and provokes an increase in the like-free OD/OH vibrators at the expenses of the "linear" ones. As the salt concentration increases, the wavenumber of these oscillators decreases (see Fig. 14), which is evidence that some H-bonding is established between  $\text{ClO}_4^-$  and water molecules and, hence, "interstitial" OH/OD oscillators are really very weak or not at all bonded oscillators.

The evolution of the BHB ( $2587\text{ cm}^{-1}$ ) band in both salts deserves comment. Although the bands' parameters of this component are difficult to estimate accurately because of the great overlapping with

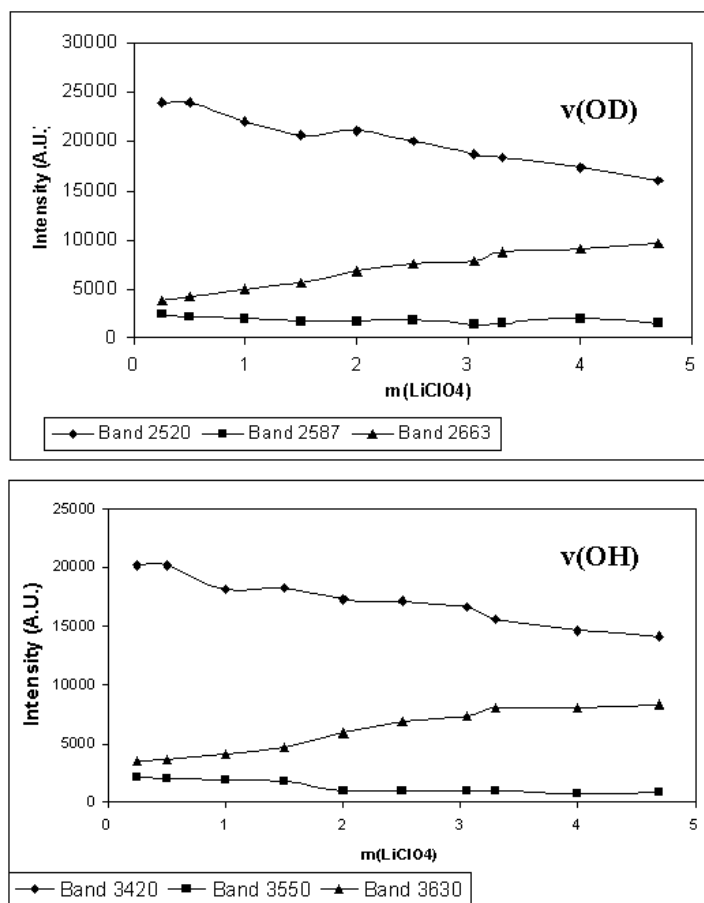


**Fig. 13** Dependence with  $\text{LiClO}_4$  concentration of the band intensity of the three components found by deconvolution in the  $\nu(\text{OD})/\nu(\text{OH})$  stretching vibrations of  $\text{D}_2\text{O}/\text{H}_2\text{O}$  1:1 mixture.

the main band at  $2520\text{ cm}^{-1}$ , their intensities follow, in general, the same behavior. This means that linear and BHB local structures are closely related, and the perturbation of the former implies the perturbation of the second. Nevertheless, the wavenumbers appear to be little perturbed in both cases.

## CONCLUSIONS

A detailed Raman spectroscopic study has been performed in aqueous solutions of  $\text{LiCl}$  and  $\text{LiClO}_4$  salts in  $\text{D}_2\text{O}/\text{H}_2\text{O}$  mixtures. Prior to that, a study of the vibrational characteristics of the isotopic mixture was necessary to analyze the main components present in the spectrum and their dependence on concentration, which was performed by using Fourier transform self-deconvolution methods and fitting methods. In the diluted case, where the inter- and intramolecular couplings do not play any appreciable role, it appears that  $\nu(\text{OD})/\nu(\text{OH})$  are composed of three bands at  $2520$ ,  $2587$ , and  $2666\text{ cm}^{-1}$ , which are assigned respectively to linear, bifurcated, and almost-free OD/OH oscillators (“interstitial” oscillators), the relative concentration of which remain constant as a function of the  $\text{D}_2\text{O}/\text{H}_2\text{O}$  ratio. This implies that the water spectrum can be considered a mixture of three spectroscopically detectable local configurations. As concentration rises, a new band appears at  $2370\text{ cm}^{-1}$  ( $3280\text{ cm}^{-1}$ ) as a consequence of these couplings.

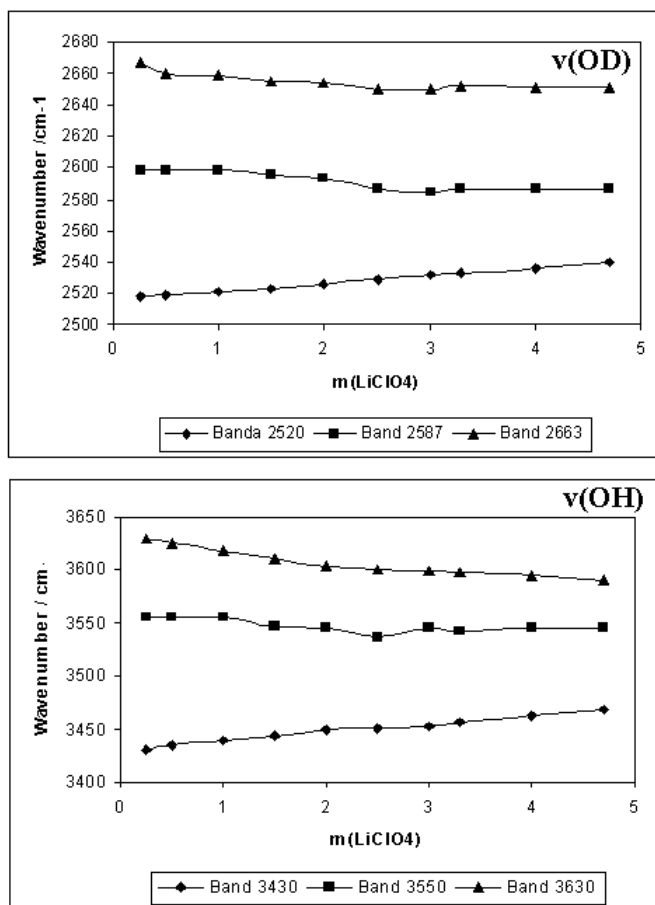


**Fig. 14** Wavenumber dependence of the components of  $\nu(\text{OD})$  and  $\nu(\text{OH})$  bands with  $\text{LiClO}_4$  concentration in a  $\text{D}_2\text{O}/\text{H}_2\text{O}$  1:1 mixture.

The addition of salts to 1:1 isotopic mixtures induces different perturbations in these bands.  $\text{LiCl}$  disturbs all the couplings and also affects the linear H-bonds, which are modified to  $\text{OH}\cdots\text{Cl}$  bonds with H-bond energy a little weaker than  $\text{OH}\cdots\text{O}$  energy. Nevertheless, this salt does not greatly affect the interstitial H-bonds.

$\text{LiClO}_4$  also disturbs all the couplings, but its effect is mainly to radically modify the linear H-bond, which becomes a very weak H-bond. Nevertheless, these  $\text{OH}\cdots\text{ClO}_4^-$  bonds are stronger than the interstitial H-bonds in bulk water.

## REFERENCES

1. N. Ohtomo, K. Tokiwano, K. Arakawa. *Bull. Chem. Soc. Jpn.* **54**, 1802 (1981).
2. G. Walrafen. "Raman and infrared spectral investigations of water structure", in *Water: A Comprehensive Treatise*, Vol. I, F. Frank (Ed.), Plenum, London (1972).
3. I. P. Gibson and J. C. Dore. *Mol. Phys.* **48**, 1019 (1983).
4. A. Rahman and F. H. Stillinger. *J. Chem. Phys.* **55**, 3336 (1971).
5. D. W. Wood. "Computer simulations of water and aqueous solutions", in *Water: A Comprehensive Treatise*, Vol. VI, F. Frank (Ed.), Plenum, London (1979).

6. I. M. Svishchev and P. G. Kusalik. *J. Chem. Phys.* **99**, 3049 (1993).
7. D. Bernal and R. H. Fowler. *J. Chem. Phys.* **1**, 515 (1933).
8. V. Gutmann, E. Plattern, G. Resh. *Chimia* **31**, 431 (1977).
9. A. Ben-Naim. *J. Chem. Phys.* **57**, 3650 (1972).
10. C. M. Davis and T. A. Litovitz. *J. Chem. Phys.* **42** (7), 2563 (1965).
11. Yu. Ya. Efimov and Yu. I. Naberukhin. *Mol. Phys.* **30**, 1621 (1975).
12. Yu. Ya. Efimov and Y. I. Naberukhin. *Faraday Discuss. Chem. Soc.* **85**, 117 (1988).
13. F. H. Stillinger and A. Rahman. *J. Chem. Phys.* **60**, 1545 (1974).
14. C. Pangali, M. Rao, B. J. Berne. *Mol. Phys.* **49**, 661 (1980).
15. H. Tanaka. *J. Chem. Phys.* **112**, 799 (1999).
16. C. H. Cho, J. Urquidi, G. I. Gellene, G. W. Robinson. *J. Chem. Phys.* **114**, 3157 (2001).
17. R. C. Dougherty and L. N. Howard. *J. Chem. Phys.* **109**, 7379 (1998).
18. M. Chaplin. [www.sbu.ac.uk/water/index.html](http://www.sbu.ac.uk/water/index.html)
19. K. Johnson. [www.watercluster.com](http://www.watercluster.com)
20. F. Rull and J. A. de Saja. *J. Raman Spectrosc.* **17**, 167 (1986).
21. V. Zhelyaskov, G. Georgiev, Zh. Nickolov, M. Miteva. *J. Raman Spectrosc.* **20**, 67 (1989).
22. J. Wiafe-Aketen and R. Bansil. *J. Chem. Phys.* **78**, 7132 (1983).
23. F. Rull, C. Prieto, F. Sobrón. *J. Mol. Struct.* **143**, 305 (1986).
24. T. T. Wall and D. F. Hornig. *J. Chem. Phys.* **43**, 2079 (1965).
25. W. C. Mundy, I. Gutierrez, F. H. Speeding. *J. Chem. Phys.* **59**, 2173 (1973).
26. I. Savatinova, E. Anachkova, R. Nikolaeva. *Spectrosc. Lett.* **19**, 167 (1986).
27. N. A. Chumaevskii, M. N. Rodnikova, D. A. Sirotkin. *J. Mol. Liq.* **82**, 39 (1999).
28. E. C. Clarke and D. N. Glew. *Can. J. Chem.* **50**, 16655 (1972).
29. P. A. Giguère. *J. Raman Spectrosc.* **19**, 354 (1984).
30. G. G. Malenkov, D. L. Tytik, E. A. Zheligovskaya. *J. Mol. Liq.* **82**, 27 (1999).
31. J. Dudessy, Th. Lhomme, M. C. H. Boiron, F. Rull. *Appl. Spectrosc.* **56**, 99 (2002).